Nuclear Science and Techniques (2023) 34:68
https://doi.org/10.1007/s41365-023-01217-z

Procedure for determining the number of thermal diffusion columns in square cascade for separation of Ne stable isotopes

Fatemeh Mansourzadeh[1] · Mohammad Mahdi Shadman[1] · Javad Karimi Sabet[1] · Valiyollah Ghazanfari[1]

Received: 12 October 2022 / Revised: 4 March 2023 / Accepted: 6 March 2023 / Published online: 13 May 2023

Abstract

The thermal diffusion column represents one method of separating stable isotopes. This method is advantageous for small-scale operations because of the simplicity of the apparatus and small inventory, especially in gas-phase operations. Consequently, it has attracted attention for its applicability in tritium and noble gas separation systems. In this study, the R cascade was used to design and determine the number of columns. A square cascade was adopted for the final design because of its flexibility, and calculations were performed to separate ^{20}Ne and ^{22}Ne isotopes. All the R cascades that enriched the Ne isotopes by more than 99% were investigated, the number of columns was determined, and the square cascade parameters were optimized using the specified columns. Additionally, a calculation code "RSQ_CASCADE" was developed. A unit separation factor of three was considered, and the number of studied stages ranged from 10 to 20. The results showed that the column separation power, relative total flow rate, and required number of columns were linearly related to the number of stages. The separation power and relative total flow decreased and the number of columns increased as the stage number increased. Therefore, a cascade of 85 columns is recommended to separate the stable Ne isotopes. These calculations yielded a 17-stage square cascade with five columns in each stage. By changing the stage cut, feed point, and cascade feed flow rate, the best parameters for the square cascade were determined according to the cascade and column separation powers. As the column separation power had a maximum value in cascade feed 50, it was selected for separating Ne isotopes.

Keywords Stable isotope · Thermal diffusion · Cascade · Separation · Neon

1 Introduction

Stable isotopes are widely applied as precursors for radioisotopes and used in fields such as medicine, electronics, mineral exploration, metallurgy, industry, and physics research [1, 2]. Understanding separation techniques would facilitate the production of a substantial of stable isotopes. Thermal diffusion is an important process because of its positive attributes, such as a high separation coefficient, simplicity, and cascade operation. Moreover, the apparatus involved is advantageous for small-scale operation because of its simplicity and small inventory, particularly for gas-phase operations. Consequently, it has attracted attention for its applicability in tritium and noble gas separation systems [3, 4]. This method produces expensive isotopes with high purity on a small scale (1–2 g of the target isotope per day at a concentration of over 99%). The temperature difference is the most crucial factor affecting mass transfer in a column. Separation using a temperature gradient was first conducted in 1938 by Classius and Dickel, who showed that high-efficiency component separation could be achieved by creating a convective flow using a temperature gradient [5]. Over an extended period, Clausius et al. separated small quantities of the stable isotopes of chlorine, nitrogen, oxygen, carbon, and successfully separated many isotopes, including ^{126}Xe (33.6%), ^{132}Xe (17.5%), ^{21}Ne (99.6%), and ^{20}Ne (99.95%) [3, 5]. Other researchers have reported successful stable isotope separation using thermal diffusion columns. In 1960, Saxena and Watson optimized the physical parameters of a thermal diffusion column [6]. In 1968, Rutherford et al. designed a column sample to compare the theoretical and experimental results of Ar, CH_4, and Xe isotope separation and utilized a six-stage cascade to separate ^{124}Xe using 24 columns [2].

✉ Fatemeh Mansourzadeh
fmansourzadeh@aeoi.org.ir

[1] Nuclear Fuel Cycle Research School, Nuclear Science and Technology Research Institute, Tehran, Iran

Subsequently, in 1969, they experimentally and theoretically studied the isotopic separation of O_2 and N_2 in a thermal diffusion column [7], and in 1970, they examined the separation of ^{21}Ne column and cascade [8]. In 1972, Roger and Rutherford designed a cascade to separate ^{85}Kr using a thermal diffusion column [9], and in 1979, Charles designed and investigated the ideal cascade of thermal diffusion [10]. In 1981, Rutherford et al. analyzed the behavior of a cascade by changing the time required to separate multicomponent isotopes [11]. In 1982, Zieger et al. optimized intermediate isotope enrichment in multicomponent systems [12]. In 2003, Vasaru studied the separation of ^{13}C in a seven-stage cascade using 19 thermal diffusion columns, and investigated the enrichment of ^{20}Ne and ^{22}Ne in an eight-stage cascade comprising eight columns and ^{86}Kr and ^{87}Kr in a 15-stage cascade of 35 columns [13]. From 1987 to 1997, Yamamoto et al. optimized parameters such as feed and pressure in a thermal diffusion column using analytical and experimental solutions for various noble gases [4, 14–17]. In 2020, Saiki et al. investigated hydrogen isotope separation via thermal diffusion in a two-dimensional cascade of numerous small cavities [18]. Furthermore, from 2014 to 2021, many researchers have studied numerical theories for multicomponent systems [19–22].

The thermal diffusion cascade was investigated in this study because of its application in noble gas isotope separation. The most notable approach to this problem involves determining the separating elements in a square cascade. Because of the importance of square cascades in separating multicomponent isotopes, determining the number of columns is necessary. To the best of our knowledge, although a considerable amount of research has been conducted, it has not been published. In the aforementioned studies, cascades with specific structures were used for isotope separation, and the number of columns for specific isotope separation was not specified.

The minimum total flow rate is the main criterion for determining the cascade stages and separation units, particularly when using analytical approaches [23]. This is a typical and efficient approach. In situations in which the separation factor is high, determining the number of separation units using a numerical method is more accurate than using an analytical method. When the difference between the analytical and numerical results is large, previous studies have suggested using the numerical method for determining the number of separation units. Notably, the error also increases when the number of isotopes increases. Therefore, numerical techniques are essential in cascade design [20].

This study investigated the main concepts involved in designing cascades for separating stable isotopes using a thermal diffusion column. This procedure was used as an example for Ne isotope separation, and the match abundance ratio cascade (R cascade) was used to estimate the number of columns required. We modified the numerical algorithm presented in Ref. [20] and compared the analytical and numerical results, after which the required parameters were determined to evaluate the number of columns in the R and square cascades. Owing to its flexibility, a square cascade was then designed using the calculated columns. By changing the stage cut, feed point, and cascade feed rate, the best parameters for the square cascade were determined according to the cascade and column separation powers. To this end, cascade modeling and design methods for thermal diffusion columns were identified, and calculation codes for the cascade design were prepared.

2 Research theories

The common R and square cascades are shown in Fig. 1. The feed mixture (F) with composition $z_{i,F}$ enters a cascade. The cascade then delivers the heavy product (W) and light

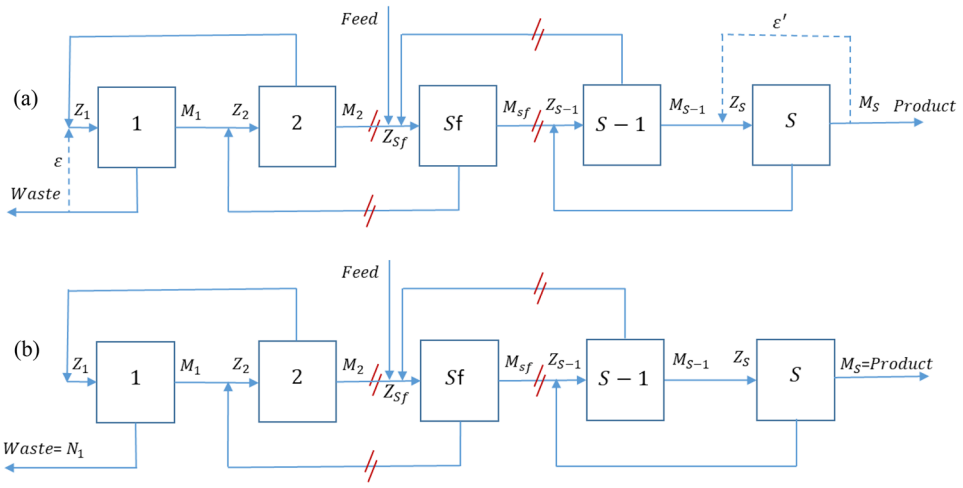

Fig. 1 **a** Square, and **b** R cascades

product (P) with compositions $x_{i,w}$ and $y_{i,p}$, respectively. Stage s receives the feed flow rate Z_s and delivers the up and down flow rates M_s and N_s, respectively [19–21].

The governing equations are listed in Table 1. The total number of stages is S, and the number of components in the feed mixture is N_c. In square cascades, the number of separation units and feed flow rate Z_s are constant in each stage (Eq. 1). In contrast to the square cascade, the rate of return flows ε and ε' in the R cascade is zero [21].

Equations 1–7 show the gas flow rates in cascade pipes [20–22]. Equations 2–5 show the mass flow balance at the mixing points from 1 to S. In these equations, the cut in each stage is θ_s. Equations 6 and 7 can be obtained using the mass flow balance in each stage and the definition of cut in stages ($\theta_s = \frac{M_s}{Z_s}$).

Equations 8–15 show the concentrations of isotopes in the cascade stages. Equation 8 shows the mass conservation of the isotope ith in the stage sth, and Eqs. 9–12 shows the mass balance of the component ith at the mixing points. $\alpha_{ij,s}$ is the separation factor between the isotopes ith and jth at the sth stage (Eq. 13), and α_0 is the overall separation factor for the unit mass difference. M_i and M_j refer to the molar weights of the ith and jth isotopes, respectively. Finally, the concentrations must satisfy the constraints in Eq. 14 [20–22], that shows the sum of the concentrations of each component at the mixing points should be equal to 1.

In the R cascade, the match abundance ratio for the two isotopes k_1 and k_2 is defined using Eq. 15 [20, 21]. The parameters R, R' and R'' are the abundance ratios in the feed, light, and heavy flows, respectively (Eq. 16). Previous studies have shown that the R cascade is suitable for thermal diffusion cascade design, such as the gas centrifuge cascade [10, 24].

The analytical approach to the R cascade is as follows [21, 23, 25]:

$$y_{i,P} = \frac{\xi_i^{s_f} - 1}{\xi_i^{N_F} - \xi_i^{-(S-s_f+1)}} z_{i,F} \Bigg/ \sum_{j=1}^{N_c} \frac{\xi_j^{s_f} - 1}{\xi_j^{N_F} - \xi_j^{-(S-s_f+1)}} z_{j,F} \tag{17}$$

$$x_{i,W} = \frac{1 - \xi_i^{-(S-s_f+1)}}{\xi_i^{s_f} - \xi_i^{-(S-s_f+1)}} z_{i,F} \Bigg/ \sum_{j=1}^{N_c} \frac{1 - \xi_j^{-(S-s_f+1)}}{\xi_j^{s_f} - \xi_j^{-(S-s_f+1)}} z_{j,F} \tag{18}$$

such that

$$\xi_i = \gamma_0^{M^* - M_i}, \text{ and } M^* = \frac{M_{k_1} + M_{k_2}}{2}. \tag{19}$$

The number of stages (S) and feed stage (s_f) with the given external isotope concentrations ($y_{k,P}, x_{k,W}$) can be obtained by solving Eqs. (17) and (18). The feed flow rate at each stage (Z_s) can be obtained using Eq. 20.

$$Z_s = \begin{cases} W \sum_{i=1}^{N_c} x_{i,W} \frac{\xi_i + 1}{\xi_i - 1} \left(\xi_i^s - 1\right), \left(1 \le s \le s_f\right) \\ P \sum_{i=1}^{N_c} y_{i,P} \frac{\xi_i + 1}{\xi_i - 1} \left(1 - \xi_i^{s-S-1}\right), \left(1 \le s \le s_f\right) \end{cases} \tag{20}$$

Based on Eq. 20, the parameter $\sum_{s=1}^{S} Z_s$ depends on ξ_i, and according to Eq. 19, ξ_i is a function of M^*. Hence, the cascade parameters for isotopes k_1 and k_2 can be determined. If M^* is used as an optimization variable and has

Table 1 Governing equations in the square and R cascades

Equation	Note	No
$Z_1 = Z_2 = \ldots = Z_S = Z$	Only in square cascade	(1)
$Z_s = M_{s-1} + N_{s+1}, s \neq s_f, s \neq S, s \neq 1$		(2)
$Z_s = M_{s-1} + N_{s+1} + F, s = s_f$		(3)
$Z_s = M_{s-1} + \varepsilon', s = S$	$\varepsilon' = 0$ in R cascade	(4)
$Z_s = N_2 + \varepsilon, s = 1$	$\varepsilon = 0$ in R cascade	(5)
$M_s = Z\theta_s$		(6)
$N_s = Z(1 - \theta_s)$		(7)
$Z_s z_{i,s} = M_s y_{i,s} + N_s x_{i,s}$		(8)
$Z_s z_{i,s} = M_{s-1} y_{i,s-1} + N_{s+1} x_{i,s+1} + F z_{i,F}, s = s_f$		(9)
$Z_s z_{i,s} = M_{s-1} y_{i,s-1} + N_{s+1} x_{i,s+1}, s \neq s_f$		(10)
$Z_s z_{i,s} - M_{s-1} y_{i,s-1} - \varepsilon' y_{i,P} = 0, s = S$	$\varepsilon' = 0$ in R cascade	(11)
$Z_s z_{i,s} - N_{s+1} x_{i,s+1} - \varepsilon x_{i,w} = 0, s = 1$	$\varepsilon = 0$ in R cascade	(12)
$\alpha_{ij,s} = \frac{(y_{i,s}/y_{j,s})}{(x_{i,s}/x_{j,s})} = \alpha_{0,s}^{(M_j - M_i)}, (i = j-1, j = 2, \ldots, N_c)$		(13)
$\sum_{i=1}^{N_c} z_{i,s} = \sum_{i=1}^{N_c} y_{i,s} = \sum_{i=1}^{N_c} x_{i,s} = 1$		(14)
$R''_{(k_1,k_2),s+1} = R_{(k_1,k_2),s} = R'_{(k_1,k_2),s-1}$	Only in R cascade	(15)
$R_{(k_1,k_2),s} = \frac{z_{k_1,n}}{z_{k_2,n}}, R'_{(k_1,k_2),s} = \frac{y_{k_1,n}}{y_{k_2,n}}, R''_{(k_1,k_2),s+1} = \frac{x_{k_1,n}}{x_{k_2,n}}$		(16)

a value between the actual components ($M_1 \le M^* \le M_{N_c}$), there is a continuous set of cascades.

2.1 Separation power

The separative power was calculated using Eq. (21).

$$\Delta U = PV_{(y_{1,P}, y_{2,P}, \ldots y_{N_c,P})} + WV_{(x_{1,W}, x_{2,W}, \ldots x_{N_c,W})} - FV_{(z_{1,F}, z_{2,F}, \ldots z_{N_c,F})} \quad (21)$$

where F, P, and W are the flows of the feed, light, and heavy products, respectively, and$y_{i,P}$, $x_{i,W}$, and $z_{i,F}$, are the corresponding isotopic concentrations. Moreover, $V(c_1, c_{2,\ldots} c_{N_c})$ is the separation potential of the multicomponent system.

There is no standard interpretation of the separation potential of multicomponent systems despite the many approaches devised for its evaluation. Thus far, relationships have been introduced for separation potentials based on different assumptions. If a small number of impurity isotopes are present in the feed and the two components are the main isotopes, the most suitable potential relation is [26].

$$V\left(c_1, c_{2,\ldots} c_{N_c}\right) = \left(\frac{\Delta M_{N_c 1}}{\Delta M_{k_1 k_2}}\right)^2 \left(c_{k_2} - c_{k_1}\right) \ln \frac{c_{k_2}}{c_{k_1}} + \sum_{\substack{k=1 \\ k \neq k_1, k_2}}^{N_c} \left(\frac{\Delta M_{N_c 1}}{\Delta M_{k_1 k}}\right)^2 c_k \ln \frac{c_k}{c_{k_1}} \quad (22)$$

where c_i is the isotopic concentration of the product, waste, or feed streams, and k_1 and k_2 are the indices of the main isotopes.

3 Calculation procedure

First, different R cascades and their effects on the separation of ^{20}Ne and ^{22}Ne were studied, and a cascade design was performed. Consequently, the required number of columns was estimated using the R cascade. Subsequently, a square cascade with specific columns was determined and optimized for the separation of Ne isotopes.

In this regard, the computational code "RSQ_CASCADE" was developed, and the required number of columns was determined to be $y_{^{20}\mathrm{Ne,P}} > 99\%$, and $x_{^{22}\mathrm{Ne,W}} > 99\%$ by changing the number of R-cascade stages from 10 to 20. The concentrations of Ne stable isotopes in the feed stream were $z_{1,F(^{20}\mathrm{Ne})} = 0.9048$, $z_{2,F(^{21}\mathrm{Ne})} = 0.0027$, and $z_{3,F(^{22}\mathrm{Ne})} = 0.0925$. The components k_1 and k_2 in the R cascade were ^{20}Ne and ^{22}Ne, respectively.

The parameters that determine the number of stages were separation power, number of columns, and relative total flow (product flow ratio to total feed flow). In this study, the unit separation factor and feed flow rate of the thermal column were 50–60 cm^3/s and 3, respectively. These parameters were obtained from experimental data [15].

The numerical procedure for the RSQ code is shown in Fig. 2. This code consists of two separate sections for modeling the R cascade (Fig. 2a) and the square cascade (Fig. 2b).

3.1 R cascade

The differences between the numerical and analytical total flow values for various alphas are listed in Table 2. When the separation factor increases, the difference between analytical and numerical methods for determining the value of $\sum Z$ increases. Therefore, we used numerical methods to calculate the separation elements. Notably, these results are for Ne isotopes, and additional changes occur as the separation factor increases for other isotopes. For example, $\sum Z/P$ for the separation of ^{78}Kr using an analytical solution was 2791.2 [25], which is equal to 2863.63 for the numerical calculation and leads to a 2.5% error. This result corresponds to a unit separation factor of 1.1. Therefore, the number of separation units was numerically determined in this study.

In the numerical approach, proportional to the initial values of the θ_s, the flow rates and the concentration of isotopes were determined based on Eqs. (2)–(7) [20]. Subsequently, nonlinear Eqs. (8)–(15) were solved using iterative methods. Therefore, the flow rates and isotope concentrations at each stage were determined. The trust-region method was used to model the R cascade and calculate the nonlinear equations. The solution method is very sensitive to preliminary guesses and often fails to find a physical solution even when the procedure converges. The continuation technique can obtain a solution with an arbitrary initial guess [20]. The R-cascade parameters were determined according to the proposed procedure using a continuation technique. For the mixing points, the value of $R^{\varepsilon(itr-1)}_{k_1 k_2, s+1}$ and $R'^{(itr-1)}_{k_1 k_2, s-1}$ in the algorithm of continuation technique was applied according to Eq. 23. The itr counts the number of iterations, and $0 < \tau < 1$ controls the speed of this transition. This allows the value of $R^{\varepsilon(itr-1)}_{k_1 k_2, s+1}$ to gradually approach that of $R'^{(itr-1)}_{k_1 k_2, s-1}$. The error was calculated using Eq. 24.

$$R'^{itr}_{k_1 k_2, s-1} - R''^{itr}_{k_1 k_2, s+1} = \left[R'^{(itr-1)}_{k_1 k_2, s-1} - R''^{(itr-1)}_{k_1 k_2, s+1}\right]\left(1 - e^{-\tau . itr}\right) \quad (23)$$

$$error = max_{s \in S}\left(\frac{\left|z_s^{(itr)} - z_s^{(\mathrm{itr}-1)}\right|}{z_s^{(n_i)}}, \frac{\left|M_s^{(n_i)} - M_s^{(n_i-1)}\right|}{M_s^{(n_i)}}, \frac{\left|N_s^{(n_i)} - N_s^{(n_i-1)}\right|}{N_s^{(n_i)}}\right) \quad (24)$$

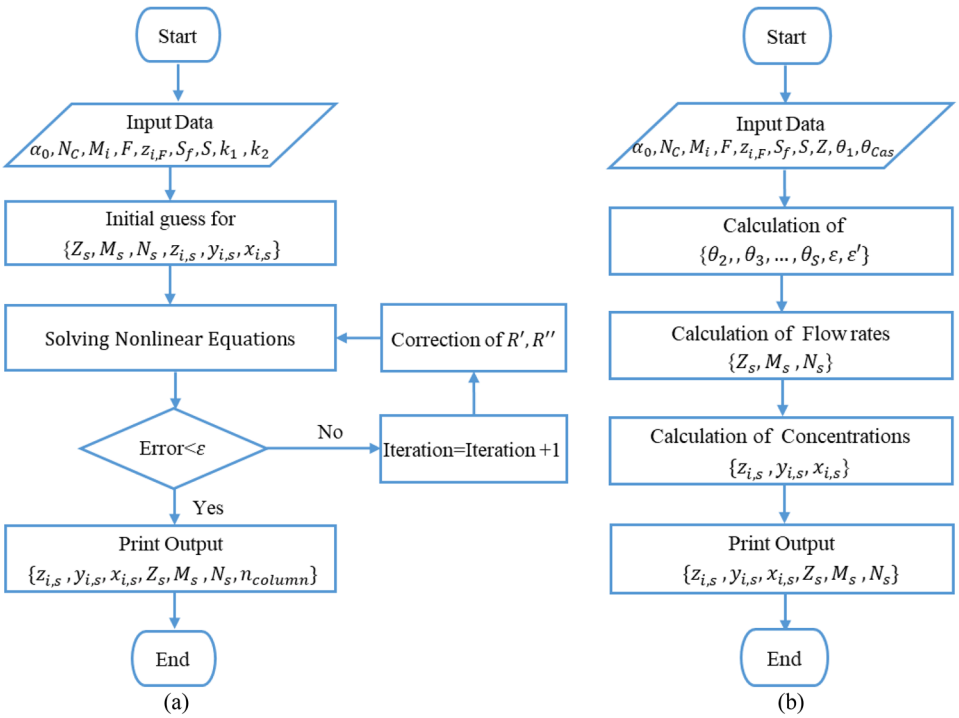

Fig. 2 Numerical procedure for **a** R cascade and **b** square cascade

Table 2 Calculated total flow rate values for the numerical and analytical methods in different alphas

α_0	1.05	1.09	1.5	2	2.5	3
$(\sum \mathbf{Z})$, Analytical	30,678.25	22,530.74	10,963.15	7044.151	5206.569	4361.049
$(\sum \mathbf{Z})$, Numerical	30,684.34	22,545.11	11,112.93	7323.95	5565.853	4791.102
error, %	0.02	0.06	1.37	3.97	6.9	9.86

The R cascade was simulated as described in Ref. [20]; however, only the solving of nonlinear equations, and the equation for the continuation technique in it is based on the Newton method and the definition of enrichment factor. A comparison of the two algorithms showed that the convergence time and number of loops required were reduced. Replacing the Newton method with a trust region and changing the homotopy equation reduced the number of required iterations from 1322 to 47. If only the trust region was used without changing the homotopy equation, the iteration convergence was reduced from 1322 to 687.

3.2 Square cascade

As mentioned before, in the simulation of the square cascade, Z_s is known and provided as the input. Moreover, the parameters M_s, N_s, ε, and ε' are unknown. Therefore, there are $2S+2$ unknown parameters. The independent equations, which include the equations of flow at the stages and mixing points, are $2S$. In solving these equations, two parameters must be determined. In a square cascade, the cut is the most significant operational parameter. Having the cut in the first stage and the cascade cut, the flow rates are obtained using Eqs. (1)–(7) [21]. Additionally, using nonlinear Eqs. (8)–(13), the concentration of isotopes is determined using the Q-iteration method explained briefly in this study.

By extracting the parameter $z_{i,s}$ from Eq. (8), and replacing it with Eqs. (9) and (10), Eqs. (25)–(28) are obtained in terms of $x_{i,s}$.

$$(M_1 q + N_1 - \varepsilon)x_{i,1} - N_2 x_{i,2} = \delta(s, S_F) F z_{i,F} \tag{25}$$

$$(N_s + M_s q)x_{i,s} - M_{s-1} q x_{i,s-1} - N_{s+1} x_{i,s-1} = \delta(s, S_F) F z_{i,F} \tag{26}$$

$$(M_P q + N_P - \varepsilon' q)x_{i,P} - M_{P-1} q x_{i,P-1} = \delta(s, S_F) F z_{i,F} \tag{27}$$

$$\delta(s, S_F) = \begin{cases} 0, (s \neq S_F) \\ 1, (s = S_F) \end{cases} \tag{28}$$

In these relations, $y_{i,s} = q_{i,s} x_{i,s}$, and considering this definition for Eq. (13), Eq. (29) is obtained as follows:

$$q_{i,s} = q_{j,s}\alpha_{0,s}^{(M_j - M_i)}. \tag{29}$$

First, the value of $q_{j,s}$ is estimated for all stages; subsequently, it is calculated in all stages using Eq. (29). Therefore, the nonlinear Eqs. (25)–(27) are linearized, and the value of $x_{i,s}$ is calculated for all stages. Subsequently, the value of $y_{i,s}$ is calculated from the definition of $q_{i,s}$. Additionally, $z_{i,s}$ is determined by considering the conservation equations for the isotope ith in the stage sth. By applying Eq. 14, the error value is checked at each calculation step, $q_{i,s}$ is modified, and the calculations are repeated. More detailed explanations are provided in Ref. [27]. Although the principles remain the same, the equations differ.

4 Results and discussion

4.1 Results for R cascade and column number estimation

The number of stages in the R cascade was changed from 10 to 20. Figure 3a shows that an increase in the number of cascade stages decreased the column separation power. This parameter varied from 27.48 to 26.95 (sccm). The column separation power for the 10-stage cascade was slightly higher than other R cascades.

As shown in Fig. 3b, the number of columns increased from 85 in the 10-stage cascade to 105 in the 20-stage cascade. Despite the increase in the number of columns and stages, the column separation power did not change considerably. Moreover, the flow rates of light and heavy products largely remained constant. However, as shown in Fig. 3c and d, the relative total flow rate decreased as the number of stages increased. The light relative total flow is $Product/\sum_{s=1}^{S} Z_s$, and the heavy relative total flow is

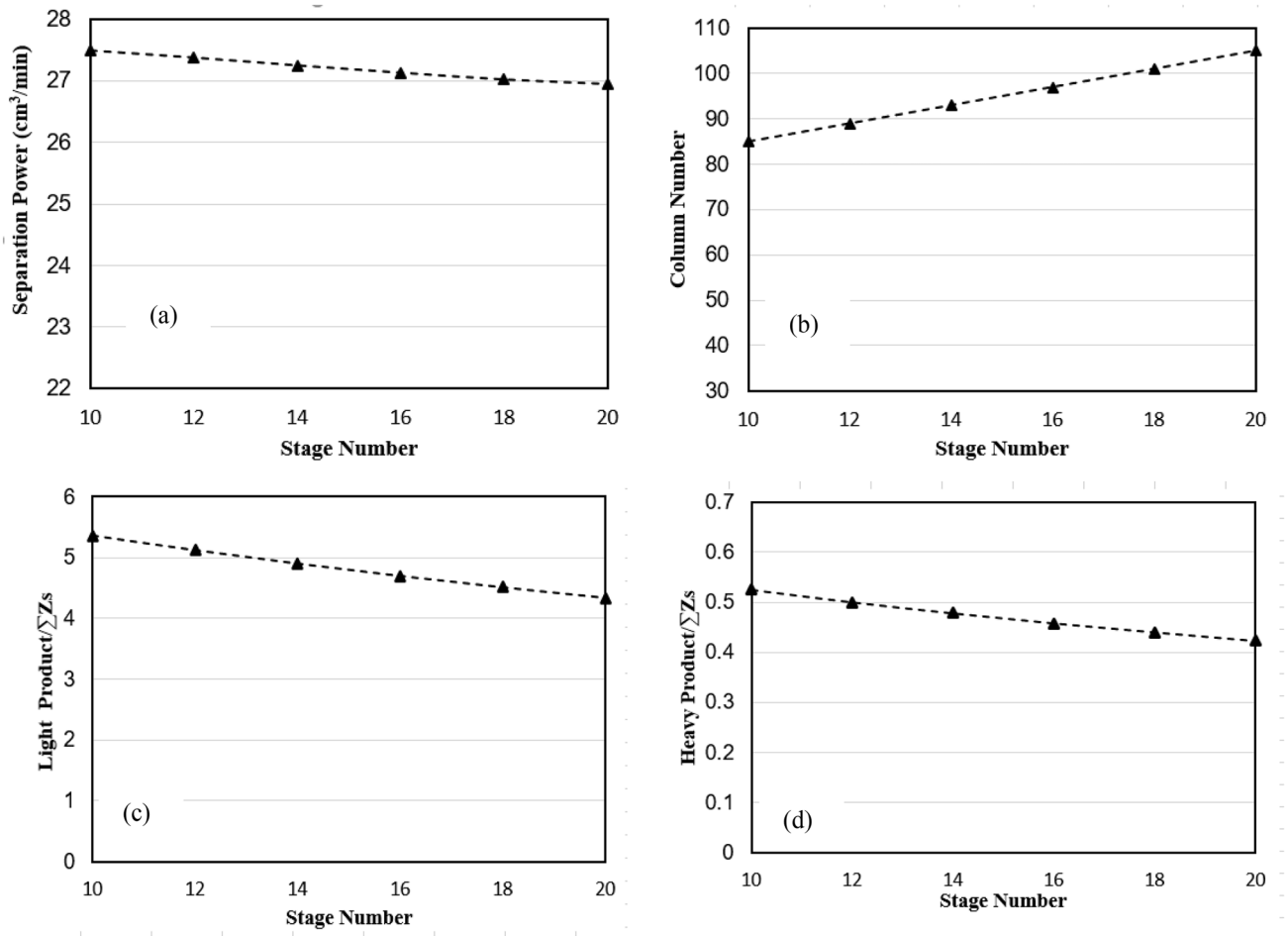

Fig. 3 **a** Column separation power, **b** column number, **c** light relative total flow, and **d** heavy relative total flow according to the number of stages

$Waste/\sum_{s=1}^{S} Z_s$. Notably, the waste in this study is related to the flow rate of the ^{22}Ne product stream that withdraws from Stage one. This phenomenon indicates that the total flow rate increases as the number of stages increased. Therefore, the best choice is a cascade with 10 stages, fewer columns, and better separation power than other R cascades. Moreover, reducing the number of columns decreases operating costs while improving separation efficiency. Therefore, because of the same light and heavy products, the same enrichment, and greater column separation power the R cascade with 85 columns was selected.

4.2 Results for square cascade

A square cascade with 85 columns was investigated based on R cascade studies. The square cascade comprised 17 stages, with five columns in each stage. By changing the θ_s, s_f, and F, the square cascade parameters were determined according to the cascade separation power and column separation power. Owing to their flexibility, these parameters in the square cascade can change each time. Table 3 presents the main parameters of the optimal squared cascade.

As mentioned above, the optimal feed rate value was 50–60 sccm. Therefore, the input flow rate for all stages was 250–300 sccm. Thus, changes could only be observed regarding θ_s, s_f, and F increasing the enrichment of both Ne-20 and Ne-22 to 99%. A suitable value for the stage cut was considered to be close to 0.5.

As the feed rate increased, the amounts of light and heavy products in the cascade increased. Moreover, with an increase in the cascade feed flow rate, the column separation power reached a maximum of 27.8 (cm^3/min) at 50 sccm and then decreased (Fig. 4a). In contrast, as shown in Fig. 4b, the cascade separation power increased as cascade feed increased. Therefore, the higher the feed rate, the better the yield and separation capacity.

In the cascade design, a pressure-regulating valve must be used at each stage to separate the desired isotopes according to the operating conditions of the column. Thus, adjusting the cut to a certain value is possible, and the separation can be performed. If the design constraints can be overcome, cascade 5 is more suitable because of its greater cascade separation power and higher product (with an increasing cascade feed rate, the cut deviation rate increases from 0.5). Otherwise, cascade 3 seems more suitable than other R cascades because of its higher column separation power.

Nevertheless, the correct and optimal use of the cascade in isotope separation depends on the preparation of the operational documentation of the column and the effects of the parameters on the separation factor.

Table 3 Main square cascade parameters

P/F	θ_N	θ_2	θ_1	Feed (sccm)	s_f	Z/F	Opt. Cascade
0.9076	0.5907	0.4908	0.5000	25	11	10	1
0.9074	0.6567	0.4946	0.4900	41.67	16	6	2
0.9075	0.6900	0.4915	0.4900	50	16	5	3
0.9075	0.7400	0.4869	0.4900	62.5	10	4	4
0.9079	0.8233	0.4792	0.4900	83.33	10	3	5

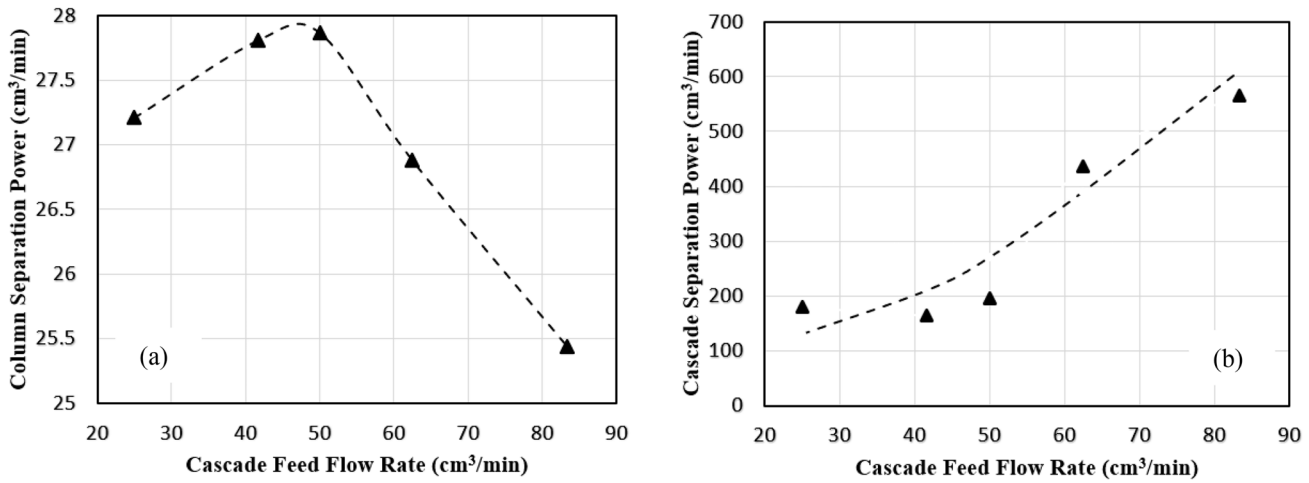

Fig. 4 Variation in **a** column separation power and **b** cascade separation power according to the square cascade feed rate

5 Conclusion

In this study, a thermal diffusion column cascade was investigated to separate Ne stable isotopes. Owing to the difference between the numerical and analytical total flow values for various alphas, numerical method to calculate the separation elements in the R cascade. Therefore, two calculation codes were developed in MATLAB. Subsequently, the thermal column separation power and the light and heavy relative total flow rates were studied in the R cascade from stages 10–20 to determine the required column numbers. The results suggest a 10-stage R cascade with 85 columns to separate stable Ne isotopes. The R cascade is better than the square cascade for separating stable Ne isotopes because of its proximity to ideal conditions. Because different cuts are required in all stages, single-column tests should be performed according to these requirements.

In the long term, in separating other isotopes of noble gases, a square cascade should be used because of its flexibility. Subsequently, a square cascade was designed, and the calculations resulted in a square cascade with 17 stages and five columns for each stage.

Conflict of interest The authors declare that they have no competing interests.

References

1. L. Chen, R. Yan, X.Z. Kang et al., Study on the production characteristics of ^{131}I and 90Sr isotopes in a molten salt reactor. Nucl. Sci. Tech. **32**, 33 (2021). https://doi.org/10.1007/s41365-021-00867-1
2. P.H. Chen, H. Wu, Z.X. Yang et al., Prediction of synthesis cross-sections of new moscovium isotopes in fusion-evaporation reactions. Nucl. Sci. Tech. **34**, 7 (2023). https://doi.org/10.1007/s41365-022-01157-0
3. W.M. Rutherford, F.W. Weyler, C.F. Eck, Apparatus for the thermal diffusion separation of stable gaseous isotopes. Rev. Sci. Instrument. **39**, 94 (1968). https://doi.org/10.1063/1.1683120
4. I. Yamamoto, M. Takakuwa, A. Kanagawa et al., Effect of operating pressure on H_2-HT separative performances of "cryogenic-wall" thermal diffusion column with continuous feed and draw-offs. J. Nucl. Sci. Technol. **28**, 321–330 (1991). https://doi.org/10.1080/18811248.1991.9731362
5. W. Furry, R.C. Jones, L. Onsager, On the theory of isotope separation by thermal diffusion. Phys. Rev. **55**, 1083 (1939). https://doi.org/10.1103/physrev.55.1083
6. S.C. Saxena, W.W. Watson, Isotope separation by a hot wire thermal diffusion column. Phys. Fluids. **3**, 105 (1960). https://doi.org/10.1063/1.1705983
7. W.M. Rutherford et al., Experimental verification of the thermal diffusion column theory as applied to the separation of isotopically substituted Nitrogen and isotopically substituted Oxygen. Chem. Phys. **50**, 5359 (1969). https://doi.org/10.1063/1.1671055
8. W.M. Rutherford, G.E. Stuber Jr, R.A. Schwind, Separation of Ne-21 from natural Neon by thermal diffusion. CONF-730915. United State (1973).
9. A. Roger, W.M. Rutherford, Design for Kr-85 enrichment by thermal diffusion, No. MLM-45342. Mound Facility, Miamisburg, OH (United States), 1972.
10. C. F. Eck, Gas phase thermal diffusion of stable isotopes, No. MLM-2659. Mound Facility, Miamisburg, OH (United States), 1979.
11. W.M. Rutherford, A Generalized computer model of the transient behavior of multicomponent isotope separation cascades. Sep. Sci. Technol. **16**, 1321–1337 (1981). https://doi.org/10.1080/01496398108058304
12. K. Zieger, G. Mueller, Optimization of the enrichment of middle components by thermal diffusion demonstrated by the example of ^{85}Kr. Isotopenpraxis **18**, 1–6 (1982)
13. G. Vasaru, Stable isotope enrichment by thermal diffusion. Rom. J. Phys. **48**, 395–406 (2003)
14. I. Yamamoto, T. Baba, A. Kanagawa, Measurement of separative characteristics of thermal diffusion column for Argon isotope separation. J. Nucl. Sci. Technol. **24**, 565–572 (1987). https://doi.org/10.1080/18811248.1987.9735847
15. I. Yamamoto, H. Makino, A. Kanagawa, Optimum pressure for total-reflux operated thermal diffusion column for isotope separation. J. Nucl. Sci. Technol. **27**, 149–156 (1990). https://doi.org/10.1080/18811248.1990.9731163
16. I. Yamamoto, H. Makino, A. Kanagawa, Optimum feed point for isotope separating thermal diffusion column. J. Nucl. Sci. Technol. **32**, 200–205 (1995). https://doi.org/10.1080/18811248.1995.9731696
17. P.G. Grodzka, B. Facemire, Clusius-dickel separation: a new look at an old technique. Sep. Sci. **12**, 103–169 (1977). https://doi.org/10.1080/00372367708058068
18. T. Saiki, N. Ono, S. Matsumoto et al., Separation of a binary gas mixture by thermal diffusion in a two-dimensional cascade of many small cavities. Inter. J. Heat. Mass. Transfer. **163**, 120394 (2020). https://doi.org/10.1016/j.ijheatmasstransfer.2020.120394
19. A.Y. Smirnov, G.A. Sulaberidze, Features of mass transfer of intermediate components in square gas centrifuge cascade for separating multicomponent mixtures. Theor. Found. Chem. Eng. **48**, 629–636 (2014). https://doi.org/10.1134/S0040579514050248
20. S. Zeng, L. Cheng, D. Jiang et al., A numerical method of cascade analysis and design for multicomponent isotope separation. Chem. Eng. Res. Des. **92**, 2649–2658 (2014). https://doi.org/10.1016/j.cherd.2013.12.016
21. F. Mansourzadeh, J. Safdari, A. Khamseh et al., Utilization of harmony search algorithm to optimize a cascade for separating multicomponent mixtures. Prog. Nucl. Energy. **111**, 165–173 (2019). https://doi.org/10.1016/j.pnucene.2018.11.005
22. S. Khooshechin, F. Mansourzadeh, M. Imani et al., Optimization of flexible square cascade for high separation of stable isotopes using enhanced PSO algorithm. Prog. Nucl. Energy. **140**, 103922 (2021). https://doi.org/10.1016/j.pnucene.2021.103922
23. T. Song, S. Zeng, G. Sulaberidze et al., Comparative study of the model and optimum cascades for multicomponent isotope separation. Sep. Sci. Technol **45**, 2113–2118 (2010). https://doi.org/10.1080/01496391003793884
24. G. Müller, G. Vasaru, The Clausius-Dickel thermal diffusion column—50 years after its invention. Isot. Environ. Healt. S. **24**, 455–464 (1988). https://doi.org/10.1080/10256018808624027
25. V. Borisevich, G. Sulaberidze, S. Zeng, New approach to optimize Q-cascades, Chem. Eng. Sci. 66 (2011). https://doi.org/10.1016/j.ces.2010.10.042

26. V.A. Palkin, Separation potential for multicomponent isotopic mixture. At. Energy **115**, 277–283 (2014). https://doi.org/10.1007/s10512-014-9783-6
27. S. Zeng, C. Ying, A robust and efficient calculation procedure for determining concentration distribution of multicomponent mixtures. Sep. Sci. Technol. **35**, 613 (2000). https://doi.org/10.1081/SS-100100179